Running head: ???

Cranial morphological disparity within the adaptive radiation of tenrecs (Afrosoricida, Tenrecidae) is no greater than expected by chance

Sive Finlay[1,2,*] and Natalie Cooper[1,2]

[1] School of Natural Sciences, Trinity College Dublin, Dublin 2, Ireland.
[2] Trinity Centre for Biodiversity Research, Trinity College Dublin, Dublin 2, Ireland.
*sfinlay@tcd.ie; Zoology Building, Trinity College Dublin, Dublin 2, Ireland.
Fax: +353 1 6778094; Tel: +353 1 896 2571.

Keywords: disparity, morphology, geometric morphometrics, tenrecs, golden moles adaptive radiation

Abstract

Introduction

Adaptive radiations, "evolutionary divergence of members of a single phylogenetic lineage into a variety of different adaptive forms" (Futuyma 1998, cited by Losos, 2010) have long-attracted the interests and attentions of naturalists. Some of the most famous examples include Darwin's finches, cichlid fish and Caribbean *Anolis* lizards (Gavrilets & Losos, 2009). These groups exhibit great variety in both species richness and phenotypic diversity. However, taxonomic diversity does not necessarily correlate with phenotypic variety (Ruta et al., 2013; Hopkins, 2013) and clades that have exceptional phenotypic diversity can still be regarded as adaptive radiations even if they are not taxonomically diverse. Therefore, to determine whether a clade has adaptively radiated it is important to test whether it exhibits exceptional (i.e. greater than expected by chance) morphological and ecological diversity (Losos & Mahler, 2010). However, few adaptive radiations have been characterised in this way.

Phenotypic diversity is commonly measured as morphological disparity; the diversity of organic form (Foote, 1997; Erwin, 2007)). There is no single definition of disparity and it can be calculated in many ways including measures of morphospace occupation (e.g. Goswami et al., 2011; Brusatte et al., 2008) and rate-based approaches that assess the amount of directed change away from an ancestor (O'Meara et al., 2006; Price et al., 2013). Analyses of disparity can be apply these alternative approaches depending on whether you are interested in current patterns of morphological diversity or the rate at which they accumulate through time.

Here we investigate current patterns of morphological disparity in

tenrecs (Afrosoricida, Tenrecidae) to determine whether they represent an adaptive radiation sensu (Losos & Mahler, 2010). Tenrecs are comprised of 34 species, 31 of which are endemic to Madagascar (Olson, 2013). From a single common ancestor (Asher & Hofreiter, 2006), Malagasy tenrecs diversified into a wide variety of descendant species which convergently resemble distantly related insectivore mammals such as shrews (*Microgale* tenrecs), moles (*Oryzorictes* tenrecs) and hedgehogs (*Echinops,Setifer* tenrecs) (Eisenberg & Gould, 1969).

Tenrecs are often cited as an example of an adaptively radiated family which exhibits exceptional morphological diversity (Soarimalala & Goodman, 2011; Olson & Goodman, 2003; Eisenberg & Gould, 1969). However, this apparent exceptional diversity is based on subjective comparisons to other groups and it has not been tested quantitatively. If tenrecs are exceptionally morphologically diverse then there are two predictions; tenrecs are more morphologically disparate than expected by chance and they are significantly more diverse than their nearest relatives, the golen moles (Afrosoricida, Chrysochloridae).

Using the most complete morphological data set of tenrecs and golden moles to date we apply geometric morphometric analyses (Rohlf & Marcus, 1993; Zelditch et al., 2012) to quantify morphological disparity among our species. Our results indicate that, on average, tenrecs are more phenotypically diverse than their closest relatives but their morphological diversity is no greater than that which is expected to evolve by chance. Therefore, under strict definitions, their designation as an exceptional adaptive radiation may need to be reconsidered.

These findings highlight the vital importance of testing our common,

but often erroneous, expectations about patterns of morphological diversity in adaptively radiated groups.

Materials and Methods

Data collection

Morphological data collection

One of us (SF) photographed cranial specimens of tenrecs and golden moles at the Natural History Museum London (NHML), the Smithsonian Institute Natural History Museum (SI), the American Museum of Natural History (AMNH), Harvard's Museum of Comparative Zoology (MCZ) and the Field Museum of Natural History, Chicago (FMNH). We photographed the specimens with a Canon EOS 650D camera fitted with an EF 100mm f/2.8 Macro USM lens using a standardised procedure to minimise potential error (see Supplementary Material for details).

We collected pictures of the skulls in dorsal, ventral and lateral views (right side of the skull) and of the outer (buccal) side of the right mandibles. A full list of museum accession numbers and access to the images can be found in the Supplementary Material.

In total we collected pictures from 182 skulls in dorsal view (148 tenrecs and 34 golden moles) and 181 mandibles in lateral view (147 tenrecs and 34 golden moles), representing 31 species of tenrec (out of the total 34 in the family) and 12 species of golden moles (out of a total of 21 in the family (Asher et al., 2010)). We used the taxonomy of Wilson and Reeder (2005) supplemented with more recent sources (IUCN, 2012;

Olson, 2013) to identify our specimens.

We used a combination of both landmarks (type 2 and type 3, (Zelditch et al., 2012)) and semilandmarks to characterise the shapes of our specimens. Our landmarks (points) and semilandmarks (outline curves) used to represent shape variation in the dorsal skulls and mandibles are in Figures 1 and 2 respectively. Corresponding landmark definitions for each view are in tables 1 and 2.

Our analyses of ventral and lateral skull views yielded similar patterns in our disparity analyses (see results), details can be found in the Supplementary Material. We digitised all landmarks and semilandmarks in tpsDIG, version 2.17 (Rohlf, 2013).

We re-sampled the outlines to a standard number of evenly spaced points which were the minimum number required to represent each outline accurately (MacLeod, 2013, details in Supplementary Material). We used TPSUtil (Rohlf, 2012) to create sliders files (Zelditch et al., 2012) which defines which points are semilandmarks. We conducted all subsequent analyses in R version 3.0.2 (R Development Core Team, 2013) within the geomorph package (Adams et al., 2013). We used the gpagen function to run a general Procrustes alignment (REFS) of the landmark coordinates while sliding the semilandmarks by minimising procrustes distance rather than bending energy (REFS). We used these Procrustes-aligned coordinates of all species (n=43) to calculate average shape values for each species which we then used for a principal components (PC) analysis (REFS) with the plotTangentSpace function (Adams et al., 2013).

Phylogeny

Instead of basing our analyses on individual trees and assuming that their topologies were known without error (e.g. Ruta et al., 2013; Foth et al., 2012; Brusatte et al., 2008; Harmon et al., 2003) we used a distribution of 101 pruned phylogenies derived from the randomly resolved mammalian supertrees in (Kuhn et al., 2011).

Eight species (six *Microgale* tenrecs and two golden moles) in our morphological data were not in the phylogenies. Phylogenetic relationships among the *Microgale* have not been resolved more recently than the (Kuhn et al., 2011) analysis, therefore we added the additional *Microgale* species at random to the *Microgale* genus within each phylogeny (Revell, 2012). We could not use the same approach to add the two missing golden mole species because they were the only representatives of their respective genera within our data. Therefore we randomly added these species to the common ancestral node (using the findMRCA function in phytools (Revell, 2012)) of all golden moles within each phylogeny. Adding these extra species to the phylogenies created polytomies which we resolved arbitrarily using zero-length branches (Paradis et al., 2004). We calculated pairwise phylogenetic distances among species using the cophenetic function (R Development Core Team, 2013).

Analyses

Disparity calculations

We calculated morphological disparity separately for golden moles and tenrecs in each of the morphological datasets. We used the PC axes which

accounted for 95% of the cumulative variation to calculate four disparity metrics; the sum and product of the range and variance of morphospace occupied by each family (Brusatte et al., 2008; Foth et al., 2012; Ruta et al., 2013). We also calculated morphological disparity directly from the Procrustes-superimposed shape data (Zelditch et al., 2012). Disparity is expected to be higher in larger groups (REFS). Therefore we repeated our disparity comparisons between the two families using rarefaction (see Supplementary Material) to confirm that observed differences in disparity between the two groups were not artefacts of differences in sample size.

To test whether tenrecs are more morphologically disparate than expected by chance, we simulated shape evolution (Harmon et al., 2008) of the species-average, Procrustes-superimposed shape coordinates of each tenrec species across our distribution of phylogenies under a Brownian Motion (BM) model (1000 simulations on each of 101 phylogenies pruned to include tenrec species only). We ran a principal components analysis on each of the simulations and used the PC axes which accounted for 95% of the cumulative variation to calculate disparity metrics.

We compared the observed disparity measure to the corresponding distribution of values and used a two-tailed test to determine whether the observed (true) disparity measures were more or less than expected by chance.

The majority of tenrecs (19 out of 31 in our data) are members of the *Microgale* (shrew-like) genus which is notable for its relatively low phenotypic diversity (Soarimalala & Goodman, 2011; Jenkins, 2003) and may mask signals of high disparity among other tenrecs. To test this we repeated our simulations of shape evolution excluding *Microgale* species.

This reduced our data from 31 to 12 species.

To test whether tenrecs are more disparate than their nearest relatives, we used a non parametric MANOVA (Anderson, 2001) to compare morphospace occupation between the two groups (REFS?).

Results

Morphological disparity in tenrecs

We compared observed disparity to calculations of disparity from BM simulations of shape data (101,000 simulations across 101 phylogenies). For each metric of disparity in both the dorsal skulls (table 3) and mandibles (table 4), the true (observed) values were significantly lower than expected compared to the distribution of simulated values. We also found significantly lower disparity than expected by chance in both the ventral and lateral skull views (Supplementary Material).

Removing the phenotypically similar *Microgale* tenrecs did not qualitatively affect our results; the non-*Microgale* tenrecs still show significantly lower phenotypic disparity than expected by chance (simulation results in the supplementary material).

Morphological disparity in tenrec and golden moles

Figures 3 and 4 depict the morphospace plots derived from our principal components analyses of average Procrustes-superimposed shape coordinates for each species in our skull and mandible data respectively. We used the principal components axes which accounted for 95% of the

cumulative variation (n = 6 axes for the dorsal skulls analysis and n = 11 axes for the mandibles) to calculate the disparity of each family.

There was agreement among all of our disparity metrics that tenrecs have more diverse dorsal skull shapes than golden moles and the two families occupy significantly different areas of morphospace.

Non-*Microgale* tenrecs also have higher disparity than golden moles and we found the same results in our analyses of ventral and lateral skull shapes (see Supplementary Material).

Surprisingly, our analyses of disparity in mandible shape yielded the opposite result; golden moles have significantly higher diversity in the shape of their mandibles than tenrecs. Again, this result is not an artifact of the relatively low phenotypic diversity within *Microgale* tenrecs; non-*Microgale* tenrecs still have significantly lower disparity in the shape of their mandibles than golden moles.

Rarefaction analyses confirmed that our findings were not the result of differences in sample size (see supplementary material).

Discussion

Our findings provide new insights into phenotypic diversity within the tenrec family. Contrary to previous suggestions (e.g. Eisenberg & Gould, 1969; Olson, 2013), tenrecs do not appear to be exceptional in their morphological diversity. They do seem to be more morphologically disparate than their closest relatives but only in skull morphology; the opposite is true when we look at mandible morphology (figure 4). Our results illustrate the vital importance of applying quantitative methods to

test assumptions about morphological diversity.

Tenrecs are evidently a diverse group, both phenotypically and ecologically. Body sizes of extant tenrecs span three orders of magnitude (2.5 to >2,000g) which is a greater range than all other Families, and most Orders, of living mammals (Olson & Goodman, 2003). Within this vast size range there is striking morphological diversity, from the spiny *Echinops, Setifer* and striking *Hemicentetes* to the shrew-like *Microgale*. Furthermore, tenrecs inhabit a variety of ecological niches and habitats including terrestrial, arboreal, semi-aquatic and semi-fossorial forms (REFS).

However, our results cast doubt over whether the evident diversity within the tenrec family should be considered to be an adaptive radiation. Phenotypic and ecological divergences within a clade are not surprising; most clades have at least small levels of disparity so, when it comes to identifying adaptive radiations, it's important to identify clades which are exceptional in their diversity (Losos & Mahler, 2010). Here we have presented the first quantitative investigation of morphological disparity in tenrecs and our results suggest that perhaps phenotypic variation in tenrecs is not the product of an adaptive radiation in the strict sense of its definition.

Although tenrecs are not more morphologically diverse than expected by chance, they do show greater cranial disparity than their nearest relatives. The discrepancies between our analyses of cranial and mandible disparity could reflect derive from factors associated with the modularity of morphological evolution.

There is strong evidence that morphological variation in skulls and

mandibles is derived from differential evolution of integrated developmental modules (reviewed by Klingenberg, 2013). For example, there seems to be two primary modules in the mouse mandible; an alveolar part which holds the teeth and the ascending ramus for muscle attachment and which articulates with the skull (Klingenberg, 2008). Geometric shape covariation is stronger within rather than between these modules.

Our landmarks and curves for the mandibles (figure 2, table 2) include aspects of variation in the dentition but they focus particular attention on the ascending ramus (condyloid, condylar and angular processes). Therefore the higher morphological disparity in golden mole mandibles most likely reflects greater variation in the shape of the muscle attachment areas of the mandible. In contrast it proved impossible to position reliable landmarks on the corresponding articulation areas of the skull in lateral view (see Supplementary).

If variation in muscle attachment/articulation sites is driving morphological disparity in mandibles, it is not clear why golden moles should have more disparate articular rami than tenrecs.

While our findings cast doubt on the designation of tenrecs as an adaptive radiation sensu (Losos & Mahler, 2010), there are certain caveats to consider which could modify the interpretation of our results.

Phenoypic variation can evolve for reasons other than adaptive radiation. Therefore, to describe phenotypic divergence as the product of an adaptive radiations requires exceptional morphological diversity in traits which have specific and proven adaptive significance (Losos & Mahler, 2010). The evolution of cranial shape (both upper skull and

mandible), particularly dental morphology, has obvious correlations with dietary specialisations (REFS) and occupation of specific ecological niches (REFS).

Considering the wide ecological diversity of our study species; the fossorial golden moles and semi-fossorial, arboreal, terrestrial and semi-aquatic tenrecs (REFS) it is reasonable to expect that variation in cranial shape should be an adaptive characterstic which allows the animals to survive in their divergent niches. Therefore quantifying the diversity of cranial morphology is a reasonable method of assessing the significance of morphological variety within the context of identifying an adaptive radiation.

Cranial shape similarities are commonly used to delineate species boundaries (REFS) or for cross-taxonomic comparative studies of phenotypic (dis)similarities (REFS). However, disparity studies are inevitably constrained to be measures of diversity within specific traits rather than overall morphology (Roy & Foote, 1997). Therefore it is possible that other morphological proxies of phenotype; analyses of linear measurements and/or discrete characters of either cranial or post-cranial morphologies could yield different results.

However, the results of (Foth et al., 2012) are encouraging. In an analysis of morphological disparity in pterosaurs, they found that disparity calculations based on geometric morphometric characterisation of skull shape yielded broadly similar results compared to analyses of whole-skeleton discrete characters and limb proportion data sets. Therefore the disparity patterns we find here based on geometric morphometric analyses of cranial shape most likely represent

approximations of disparity which are accurate for morphological diversity in the clades.

Acknowledgements

We thank the members of NERD club for insightful discussions and the musuem staff and curators for their support and access to collections. Funding was provided by an Irish Research Council EMBARK Initiative Postgraduate Scholarship (SF) and the European Commission CORDIS Seventh Framework Programme (FP7) Marie Curie CIG grant. Proposal number: 321696 (NC)

References

Adams, D., Otárola-Castillo, E. & Paradis, E. 2013. geomorph: an r package for the collection and analysis of geometric morphometric shape data. *Methods in Ecology and Evolution* **4**: 393–399. 10.1111/2041-210X.12035.

Anderson, M. 2001. A new method for non-parametric multivariate analysis of variance. *Austral Ecology* **26**: 32–46. 10.1111/j.1442-9993.2001.01070.pp.x.

Asher, R. & Hofreiter, M. 2006. Tenrec phylogeny and the noninvasive extraction of nuclear DNA. *Systematic Biology* **55**: 181–194.

Asher, R.J., Maree, S., Bronner, G., Bennett, N., Bloomer, P., Czechowski, P., Meyer, M. & Hofreiter, M. 2010. A phylogenetic estimate for golden

moles (Mammalia, Afrotheria, Chrysochloridae). *BMC Evolutionary Biology* **10**: 1–13.

Brusatte, S., Benton, M., Ruta, M. & Lloyd, G. 2008. Superiority, competition and opportunism in the evolutionary radiation of dinosaurs. *Science* **321**: 1485–1488.

Eisenberg, J.F. & Gould, E. 1969. The Tenrecs: A Study in Mammalian Behaviour and Evolution. *Smithsonian Contributions to Zoology* **27**: 1–152.

Erwin, D. 2007. Disparity: morphological pattern and developmental context. *Palaeontology* **50**: 57–73.

Foote, M. 1997. The evolution of morphological diversity. *Annual Review of Ecology and Systematics* **28**: 129–152.

Foth, C., Brusatte, S. & Butler, R. 2012. Do different disparity proxies converge on a common signal? Insights from the cranial morphometrics and evolutionary history of *Pterosauria* (Diapsida: Archosauria). *Journal of Evolutionary Biology* **25**: 904–915. 10.1111/j.1420-9101.2012.02479.x.

Gavrilets, S. & Losos, J. 2009. Adaptive radiation: contrasting theory with data. *Science* **323**: 732–736. 10.1126/science.1157966.

Goswami, A., Milne, N. & Wroe, S. 2011. Biting through constraints: cranial morphology, disparity and convergence across living and fossil carnivorous mammals. *Proceedings of the Royal Society B: Biological Sciences* **278**: 1831–1839. 10.1098/rspb.2010.2031.

Harmon, L., Schulte, J., Larson, A. & Losos, J.B. 2003. Tempo and mode of evolutionary radiation in iguanian lizards. *Science* **301**: 961–964.

Harmon, L., Weir, J., Brock, C., Glor, R. & Challenger, W. 2008. GEIGER: investigating evolutionary radiations. *Bioinformatics* **24**: 129–131.

Hopkins, M. 2013. Decoupling of taxonomic diversity and morphological disparity during decline of the Cambrian trilobite family *Pterocephaliidae*. *Journal of Evolutionary Biology* **26**: 1665–1676. 10.1111/jeb.12164.

IUCN 2012. International Union for Conservation of Nature.

Jenkins, P. 2003. *Microgale, shrew tenrecs*, pp. 1273–1278. The University of Chicago Press, Chicago.

Klingenberg, C. 2008. Morphological integration and developmental modularity. *Annual review of ecology, evolution, and systematics* **39**: 115–132.

Klingenberg, C. 2013. Cranial integration and modularity: insights into evolution and development from morphometric data. *Hystrix, the Italian Journal of Mammalogy* **24**: 43–58.

Kuhn, T., Mooers, A. & Thomas, G. 2011. A simple polytomy resolver for dated phylogenies. *Methods in Ecology and Evolution* **2**: 427–436. 10.1111/j.2041-210X.2011.00103.x.

Losos, J. 2010. Adaptive radiation, ecological opportunity, and evolutionary determinism. American Society of Naturalists E. O. Wilson Award Address. *The American Naturalist* **175**: 623–639. 10.1086/652433.

Losos, J.B. & Mahler, D. 2010. *Adaptive radiation: the interaction of ecological opportunity, adaptation and speciation*, chap. 15, pp. 381–420. Sinauer Association, Sunderland, MA.

MacLeod, N. 2013. Landmarks and semilandmarks: Difference without meaning and meaning without difference.

Olson, L. & Goodman, S. 2003. *Phylogeny and biogeography of tenrecs*, pp. 1235–1242. The University of Chicago Press, Chicago.

Olson, L.E. 2013. Tenrecs. *Current Biology* **23**: R5–R8.

O'Meara, B., Ané, C., Sanderson, M. & Wainwright, P. 2006. Testing for different rates of continuous trait evolution using likelihood. *Evolution* **60**: 922–933. 10.1111/j.0014-3820.2006.tb01171.x.

Paradis, E., Claude, J. & Strimmer, K. 2004. Ape: Analyses of Phylogenetics and Evolution in R language. *Bioinformatics* **20**: 289–290. 10.1093/bioinformatics/btg412.

Price, S., Tavera, J., Near, T. & Wainwright, P. 2013. Elevated rates of morphological and functional diversification in reef-dwelling haemulid fishes. *Evolution* **67**: 417–428. 10.1111/j.1558-5646.2012.01773.x.

Revell, L. 2012. phytools: an R package for phylogenetic comparative biology (and other things). *Methods in Ecology and Evolution* **3**: 217–223.

Rohlf, F. 2012. Tpsutil.

Rohlf, F. 2013. Tpsdig2 ver 2.17.

Rohlf, J. & Marcus, L. 1993. A revolution in morphometrics. *Trends in Ecology & Evolution* **8**: 129–132.

Roy, K. & Foote, M. 1997. Morphological approaches to measuring biodiversity. *Trends in Ecology & Evolution* **12**: 277–281.

Ruta, M., Angielczyk, K., Fröbisch, J. & Benton, M. 2013. Decoupling of morphological disparity and taxic diversity during the adaptive radiation of anomodont therapsids. *Proceedings of the Royal Society B: Biological Sciences* **280**: 20131071. 10.1098/rspb.2013.1071.

Soarimalala, V. & Goodman, S. 2011. *Les petits mammiferes de Madagascar*. Guides sur la diversité biologique de Madagascar. Association Vahatra, Antananarivo, Madagascar.

Team, R.D.C. 2013. R: A language and environment for statistical computing.

Wilson, D. & Reeder, D. 2005. *Mammal species of the world. A taxonomic and geographic reference (3rd ed)*. Johns Hopkins University Press.

Zelditch, M., Swiderski, D. & Sheets, D. 2012. *Geometric Morphometrics for Biologists, second edition*. Academic Press, Elsevier, United States of America.

List of Figures

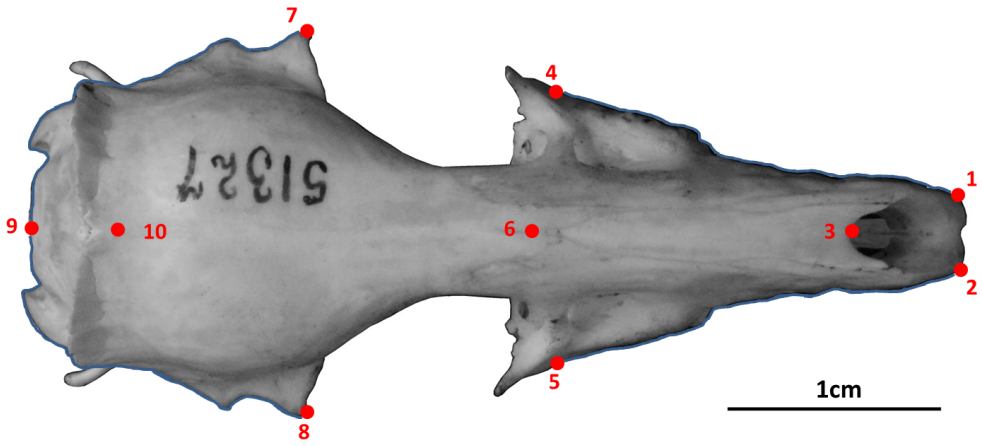

Figure 1: Landmarks (red points) and curves (blue lines) used to capture the morphological shape of skulls in dorsal view. Curves were re-sampled to the same number of evenly-spaced points. See table X for description of curves and landmarks.*Potamogale velox* (Tenrecidae) skull, accession number: AMNH_51327

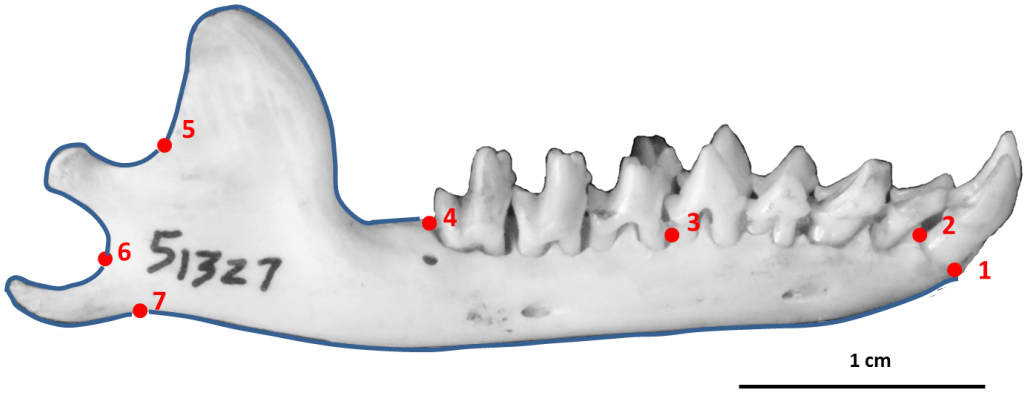

Figure 2: Landmarks (red points) and curves (blue lines) used to capture the morphological shape of mandibles. Curves were re-sampled to the same number of evenly-spaced points. See table X for description of curves and landmarks.*Potamogale velox* (Tenrecidae) mandible, accession number: AMNH_51327

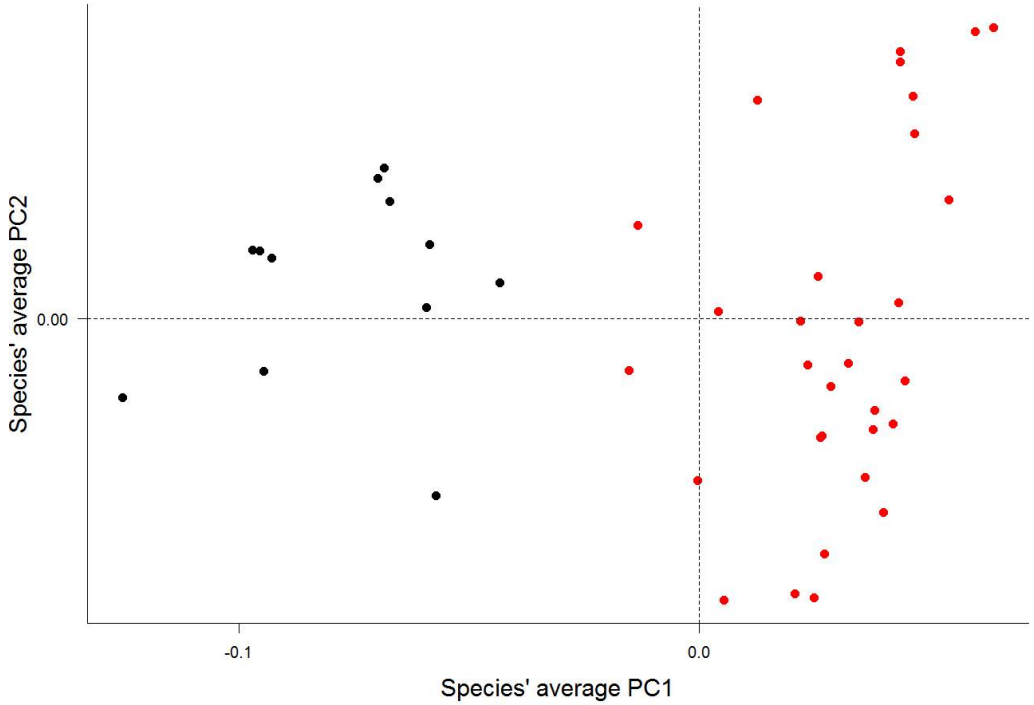

Figure 3: Principal components plot of the dorsal skulls' morphospace occupied by tenrecs (red, n=31) and golden moles (black, n=12). Axes are PC1 and PC2 of the average scores from a PCA analysis of mean Procrustes shape coordinates for each species.

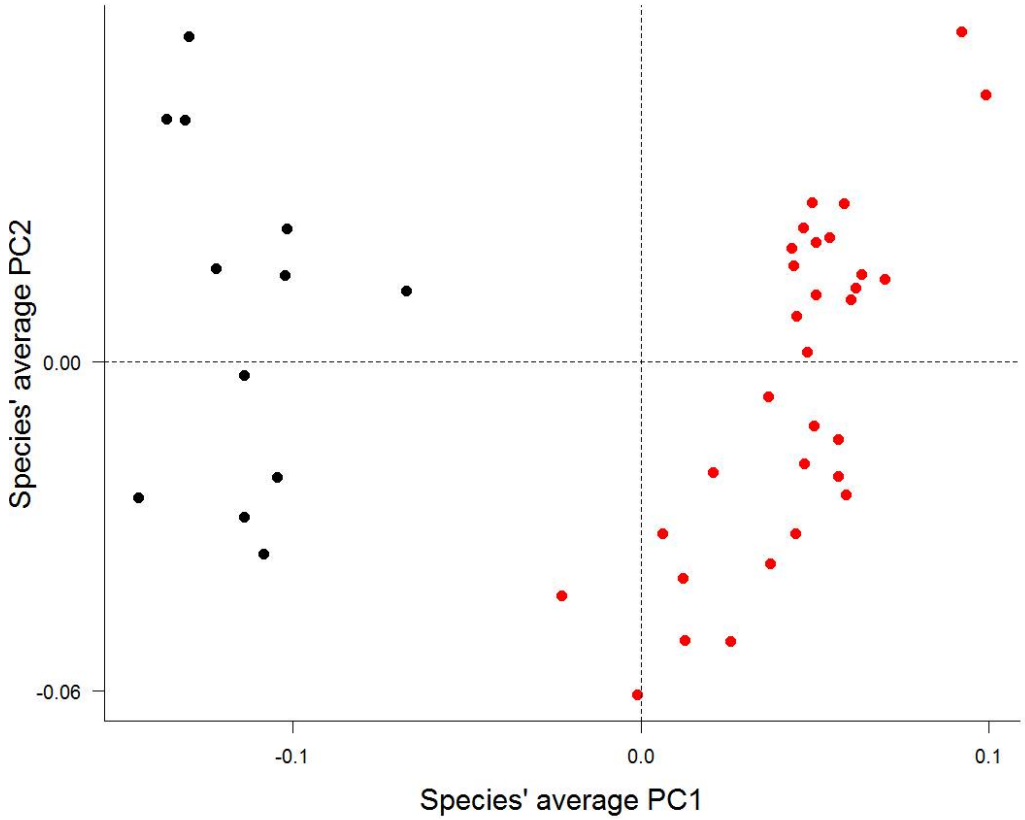

Figure 4: Principal components plot of the mandibles' morphospace occupied by tenrecs (red, n=31) and golden moles(black, n=12). Axes are PC1 and PC2 of the average scores from a PCA analysis of mean Procrustes shape coordinates for each species.

List of Tables

Table 1: Descriptions of the landmarks (points) and curves (semilandmarks) for the skulls in dorsal view (see Figure 1).

Landmark	**Description**
1 + 2	Left (1) and right (2) anterior points of the premaxilla
3	Anterior of the nasal bones in the midline
4 + 5	Maximum width of the palate (maxillary) on the left (4) and right (5)
6	Midline intersection between nasal and frontal bones
7 + 8	Widest point of the skull on the left (7) and right (8)
9	Posterior of the skull in the midline
10	Posterior intersection between saggital and parietal sutures
Curve A	Outline of the braincase on the left side, between landmarks 9 and 7
(12 points)	(does not include visible features from the lower (ventral) side of the skull)
Curve B	Outline of the palate on the left side, between landamarks 4 and 1
(10 points)	(outline of the rostrum only, not the shape of the teeth)
Curve C	Outline of the braincase on the right side, between landmarks 9 and 8
(12 points)	(does not include visible features from the lower (ventral) side of the skull)
Curve D	Outline of the palate on the right side, between landamarks 5 and 2
(10 points)	(outline of the rostrum only, not the shape of the teeth)

the text

Table 2: Descriptions of the landmarks (points) and curves (semilandmarks) for the mandibles in lateral (buccal) view (see figure 2)

Landmark	**Description**
1	Anterior of the alveolus of the first incisor
2	Posterior of the alveolus of the first incisor
3	Anterior of the alveolus of the first molar
4	Posterior of the alveolus of the last molar
5	Maximum curvature between the coronoid and condylar processes
6	Maximum curvature between the condylar and angular processes
7	Maximum curvature between the angular process and the horizontal ramus
Curve A	Condyloid process (between landmarks 4 and 5, 15 points)
Curve B	Condylar process (between landmarks 5 and 6, 15 points)
Curve C	Angular process (between landmarks 6 and 7, 15 points)
Curve D	Base of the jaw (between landmarks 7 and 1, 12 points)

Table 3: Comparison of observed and simulated disparity measures for the dorsal skulls analysis; observed (true) disparity measures, minimum simulated value (sim.min), maximum simulated value (sim.max), standard deviation of the simulated values (sdev.sim) and p value comparing the observed disparity measures to the distribution of simulated values)

Disparity metric	**Observed**	**Sim.min**	**Sim.max**	**Sdev.sim**	**p value**
Sum of Variance	0.0017	24742.44	286028.06	20878.99	0
Product of Variance	0.00013	1306.57	286028.06	3518.66	0
Sum of Ranges	0.38	1224.51	2934.11	167.54	0
Product of Ranges	0.047	148.62	1627.71	60.48	0

Table 4: Comparison of observed and simulated disparity measures for the mandibles analysis; observed (true) disparity measures, minimum simulated value (sim.min), maximum simulated value (sim.max), standard deviation of the simulated values (sdev.sim) and p value comparing the observed disparity measures to the distribution of simulated values)

Disparity metric	**Observed**	**Sim.min**	**Sim.max**	**Sdev.sim**	**p value**
Sum of Variance	0.0032	23459.28	286827.19	20915.32	0
Product of Variance	0.000189	1173.95	286827.19	3346.28	0
Sum of Ranges	0.676	1212.44	2996.77	170.86	0
Product of Ranges	0.0639	151.54	1520.68	60.51	0